

Interplay between sign problem and Z_3 symmetry in three-dimensional Potts models

Takehiro Hirakida,^{1,*} Hiroaki Kouno,^{2,†} Junichi Takahashi,^{1,‡} and Masanobu Yahiro^{1,§}

¹*Department of Physics, Graduate School of Sciences, Kyushu University, Fukuoka 819-0395, Japan*

²*Department of Physics, Saga University, Saga 840-8502, Japan*

(Received 8 April 2016; published 8 July 2016)

We construct four kinds of Z_3 -symmetric three-dimensional (3D) Potts models, each with a different number of states at each site on a 3D lattice, by extending the 3D 3-state Potts model. Comparing the ordinary Potts model with the four Z_3 -symmetric Potts models, we investigate how Z_3 symmetry affects the sign problem and see how the deconfinement transition line changes in the μ - κ plane as the number of states increases, where μ (κ) plays a role of chemical potential (temperature) in the models. We find that the sign problem is almost cured by imposing Z_3 symmetry. This mechanism may happen in Z_3 -symmetric QCD-like theory. We also show that the deconfinement transition line has stronger μ dependence with respect to increasing the number of states.

DOI: 10.1103/PhysRevD.94.014011

I. INTRODUCTION

Thermodynamic properties of quantum chromodynamics (QCD) are often described as a phase diagram in the μ - T plane, where T and μ mean temperature and quark-number chemical potential, respectively. However, the QCD phase diagram is known only in the vicinity of the T axis, because lattice QCD (LQCD) simulations as the first principle calculation have a serious sign problem at finite real μ . Exploration of the QCD phase diagram then becomes one of the most challenging subjects in particle and nuclear physics, and the results have been playing an important role in cosmology and astrophysics. The quark determinant, which appears after the quark field is integrated out in the grand-canonical QCD partition function in the Euclidean path integral formalism, becomes complex for finite real μ . Several approaches have been proposed so far to resolve this sign problem, such as the reweighting method [1], the analytic continuation from imaginary μ to real μ [2–7], and the Taylor expansion method [8,9]. Recently, remarkable progress has been made in the complex Langevin simulation [10–14] and the Picard-Lefschetz thimble theory [15–17], but our understanding is still far from perfection.

Z_3 symmetry is exact in pure gauge theory but not in QCD with finite quark masses. However, the symmetry is considered to work well as an approximate symmetry and be related to the deconfinement transition. It was pointed out that the Z_3 symmetry or group may play an important role in the sign problem. In Refs. [18] and [19], it was shown that, using the properties of Z_3 group elements, an effective center field theory with sign problem can be

transformed into a flux model with no sign problem. It was also conjectured that the center-dressed quarks undergo a new phase due to the Fermi-Einstein condensation in cold but dense matter of the hadronic phase and the phenomena are key to the solution of the sign problem [20]. Recently, in Ref. [21], it was suggested that, even in the case of the full QCD having Z_3 symmetry approximately, the sign problem may be cured to some extent by using the Z_3 -averaged subset method, at least in the strong coupling limit. However, there are still many difficulties, when the methods are applied to realistic full LQCD simulations.

As mentioned above, in pure SU(3) gauge theory, Z_3 symmetry is exact and characterizes the confinement-deconfinement transition. The Polyakov loop $L(\mathbf{x})$ [22], not invariant under the Z_3 transformation, is an order parameter of the transition. The expectation value $\langle L(\mathbf{x}) \rangle$ is also related with the free energy of a static quark. If $\langle L(\mathbf{x}) \rangle = 0$, the free energy becomes infinite and thereby quarks are confined. In the full QCD with dynamical quarks, however, Z_3 symmetry is not exact anymore and the relation between Z_3 symmetry and the confinement-deconfinement transition is not clear.

In a series of papers [23–27], Z_3 -symmetric QCD-like theory was proposed and studied extensively. In this paper, we simply refer to the theory as Z_3 -QCD. In Z_3 -QCD, the symmetric three flavor quarks are considered and the flavor dependent imaginary chemical potential is introduced to retain Z_3 symmetry. In the papers, the phase structure in the Z_3 -QCD was studied by using the Polyakov-loop extended Nambu–Jona-Lasinio (PNJL) model [28–32] as an effective model of QCD. Recently, lattice simulations of Z_3 -QCD was done at $\mu = 0$ [33]. The result was shown to be consistent with the PNJL-model prediction. It should be also remarked that the Z_3 -QCD tends to three flavor QCD in the limit of $T \rightarrow 0$ as is explained in next section.

*hirakida@email.phys.kyushu-u.ac.jp

†kounoh@cc.saga-u.ac.jp

‡takahashi@phys.kyushu-u.ac.jp

§yahiro@phys.kyushu-u.ac.jp

There is a possibility that the sign problem becomes milder in Z_3 -QCD than in QCD. Kouno *et al.* pointed out this possibility by making a qualitative comparison between the heavy-dense model [13,34] and its Z_3 -symmetric extension newly constructed, and proposed a Taylor-expansion method of deriving QCD results from Z_3 -QCD ones [27]. The interplay between the sign problem and Z_3 symmetry is thus quite interesting.

The heavy-dense model is well known as an effective model of QCD for large mass M and large μ keeping $\mu - M$ is finite. The three-dimensional (3D) three-state Potts model [18,19,35–37] is a simplified version of the heavy-dense model. In this sense, the Potts model should be considered at large M and μ . In the Potts model, three elements ($1, \exp[\pm i2\pi/3]$) of the group Z_3 are taken as three states at each site on a 3D lattice. Considering the Z_3 elements as a substitute for the Polyakov-loop operator $L(\mathbf{x})$ in QCD, one can discuss Z_3 symmetry and confinement through the 3D Potts model. In QCD, the operator $L(\mathbf{x})$ depends on the 3D coordinate \mathbf{x} and T , but in the Potts model the Z_3 elements can depend on \mathbf{x} but lose information on T as a result of the substitution. One can regard \mathbf{x} -dependent Z_3 elements as a Polyakov-loop operator $\Phi_{\mathbf{x}}$ in the 3D Potts model. The $\Phi_{\mathbf{x}}$ should be averaged over \mathbf{x} to define random and ordered states. The average $\langle \Phi \rangle$ depends on the coupling strength κ of the interaction between $\Phi_{\mathbf{x}}$ at site \mathbf{x} and those at the nearest neighbor sites. As an interesting result, κ dependence of $\langle \Phi \rangle$ in the Potts model is shown to be similar to T dependence of the Polyakov loop $\langle L(\mathbf{x}) \rangle$ in QCD [35]. This indicates that κ plays a role of temperature and one can consider the phase diagram in the μ - κ plane.

In this paper, we construct four kinds of Z_3 -symmetric 3D Potts models, each with different number of states, in order (1) to clarify the interplay between Z_3 symmetry and the sign problem, and (2) to see how the deconfinement transition line changes in the μ - κ plane with respect to increasing the number of states of $\Phi_{\mathbf{x}}$. Basic properties of the four Z_3 -symmetric 3D Potts models, (A)–(D), are tabulated in Table I, together with those of the original 3D 3-state Potts model. We clarify subject (1) by comparing the original Potts model with model (D) and subject (2) by changing the number of states from 3 of model (A) to 13 of model (D).

The Potts model is missing the chiral symmetry, because it considers the case of large quark mass. Hence, we cannot discuss the chiral phase transition directly. However, there is an onset transition of quark number density, in addition to the deconfinement transition, in the Potts model. The order parameter of the transition is, of course, the quark number density itself. As for the critical endpoint of chiral transition at finite T and μ in QCD, it was pointed out [38] that the order parameter is not the scalar density only, but a linear combination of the scalar, quark number and energy densities. This mixing makes the chiral transition the first

TABLE I. Potts and Z_3 -symmetric Potts models considered in this paper. Z_3 -symmetric Potts models (A)–(D) are classified with the number of states at each site. The definition and properties of models are shown in Sec. IV for the Potts model and in Sec. V for the Z_3 -symmetric Potts models.

Model	States	Z_3 symmetry	Free from sign problem?
Potts	3	non-symmetric	No
(A)	3	symmetric	Yes
(B)	4	symmetric	Yes
(C)	7	symmetric	Yes
(D)	13	symmetric	No

order at middle and large μ/T . In this sense, we can regard the quark number density as the quantity related to the chiral transition at middle and large μ . Similarly, the onset transition also affects the deconfinement transition. We will show that, in the Z_3 -symmetric 3D Potts model, the sign problem appears when the deconfinement transition is entangled strongly with the onset transition.

This paper is organized as follows. We recapitulate Z_3 -QCD in Sec. II. In Sec. III, we overview the sign problem and show a way of making the QCD partition function real. In Sec. IV, the sign problem in the 3D 3-state Potts model is examined. In Sec. V, we construct Z_3 -symmetric 3D Potts models. Numerical simulations are done for the models in Sec. VI. Section VII is devoted to a summary.

II. QCD AND Z_3 -QCD

As for finite T , the action S of three-flavor QCD with symmetric quark masses (m) and symmetric chemical potentials (μ) is defined by

$$S = \int_0^\beta dx_4 \int_{-\infty}^{\infty} d^3x \mathcal{L} \quad (1)$$

with $\beta = 1/T$ and the Lagrangian density

$$\mathcal{L} = \mathcal{L}_Q + \mathcal{L}_G \quad (2)$$

composed of the quark and gluon parts

$$\mathcal{L}_Q = \bar{q} \mathcal{M}(\mu, A_\mu) q, \quad (3)$$

$$\mathcal{L}_G = \frac{1}{4g^2} F_{\mu\nu}^a{}^2 = \frac{1}{2g^2} \text{Tr}[F_{\mu\nu}{}^2], \quad (4)$$

where

$$\mathcal{M}(\mu, A_\mu) = D_\mu(A_\mu) \gamma_\mu + m - \mu \gamma_4, \quad (5)$$

$$F_{\mu\nu} = \partial_\mu A_\nu - \partial_\nu A_\mu - ig[A_\mu, A_\nu], \quad (6)$$

$$A_\mu = \sum_{a=1}^8 A_\mu^a T^a. \quad (7)$$

Here q , A_μ and T^a are the quark field, the gluon field, and the generator of SU(3) group, respectively, and the trace Tr is taken for the color indices. As for T^a , we use the standard notation $T^a = \frac{\lambda^a}{2}$ defined by the Gell-Mann matrices λ^a . The action S then can be decomposed into the quark and gluon components as $S = S_Q + S_G$ with

$$\begin{aligned} S_Q &= \int_0^\beta dx_4 \int_{-\infty}^{\infty} d^3x \mathcal{L}_Q, \\ S_G &= \int_0^\beta dx_4 \int_{-\infty}^{\infty} d^3x \mathcal{L}_G. \end{aligned} \quad (8)$$

In the present formalism, we have used the following Euclidean notations:

$$\begin{aligned} x_4 &\equiv ix_0 = ix^0 = it, & A_4 &\equiv iA_0 = iA^0, \\ D_\mu(A_\mu) &= \frac{\partial}{\partial x_\mu} - iA_\mu, \\ \gamma_4 &= \gamma_M^0, & \gamma_i &\equiv i\gamma_M^i \quad (i = 1, 2, 3), \end{aligned} \quad (9)$$

where the γ_M^μ ($\mu = 0, 1, 2, 3$) are the standard gamma matrices in Minkowski space [39]. The temporal anti-periodic boundary condition on the quark field is given by

$$q(x_4 = \beta, \mathbf{x}) = -q(x_4 = 0, \mathbf{x}), \quad (10)$$

while the gluon field satisfies the temporal periodic boundary condition. The Lagrangian density \mathcal{L} is invariant under the Z_3 transformation,

$$\begin{aligned} q &\rightarrow q' = Uq, \\ A_\mu &\rightarrow A'_\mu = UA_\mu U^{-1} + i(\partial_\mu U)U^{-1}, \end{aligned} \quad (11)$$

where

$$U(x_4, \mathbf{x}) = \exp(i\alpha^a T^a) \quad (12)$$

is an element of SU(3) group characterized by real functions α^a satisfying the boundary condition

$$U(x_4 = \beta, \mathbf{x}) = \exp(-i2\pi k/3)U(x_4 = 0, \mathbf{x}) \quad (13)$$

for any integer k . However, the quark field boundary condition (10) is changed by the Z_3 transformation as

$$q(x_4 = \beta, \mathbf{x}) = -e^{i2\pi k/3}q(x_4 = 0, \mathbf{x}). \quad (14)$$

In full QCD with dynamical quarks, Z_3 symmetry is thus broken through the quark boundary condition.

Z_3 symmetry can be recovered by introducing the flavor-dependent twist boundary condition (FTBC) as follows.

$$q(x_4 = \beta, \mathbf{x}) = -e^{-i\theta_f}q(x_4 = 0, \mathbf{x}) \quad (15)$$

with

$$\theta_f = \frac{2\pi}{3}f \quad (f = -1, 0, 1). \quad (16)$$

For later convenience, the flavor indices are numbered as $-1, 0, 1$. Under the Z_3 transformation (11), the FTBC (15) is changed into

$$q_f(x_4 = \beta, \mathbf{x}) = -e^{-i\theta'_f}q_f(x_4 = 0, \mathbf{x}) \quad (17)$$

with

$$\theta'_f = \frac{2\pi}{3}(f - k) \quad (f = -1, 0, 1). \quad (18)$$

The boundary condition (17) after Z_3 transformation returns to the original one (15) by relabeling the flavor indices $f - k$ as f . Hence, if we consider the FTBC instead of the standard one in S , the QCD-like theory obviously has Z_3 symmetry. This theory is abbreviated as Z_3 -QCD in this paper.

The Z_3 -QCD tends to QCD with symmetric three flavor quarks in the limit of $T \rightarrow 0$, since the difference between the two theories comes only from the temporal fermion boundary condition that has no contribution in the limit.

When the fermion fields q_f are transformed as [40]

$$q_f \rightarrow \exp(-i\theta_f T x_4)q_f, \quad (19)$$

the boundary condition (15) returns to the ordinary one (10), but \mathcal{L} is changed into

$$\mathcal{L}^\theta = \bar{q}(\gamma_\nu D_\nu^\theta + m)q + \frac{1}{4g^2}F_{\mu\nu}^a{}^2 \quad (20)$$

with $D_\nu^\theta \equiv \partial_\nu - i(A_\nu + \hat{\theta}\delta_{\nu,4}T)$, where the flavor-dependent imaginary chemical potentials $i\hat{\theta}T$ are defined by

$$\begin{aligned} \hat{\theta} &= \text{diag}(\theta_{-1}, \theta_0, \theta_1) \\ &= \text{diag}(-2\pi/3, 0, 2\pi/3). \end{aligned} \quad (21)$$

The flavor-dependent imaginary chemical potentials partially break $SU(3)$ flavor symmetry and associated $SU(3)$ chiral symmetry [23,24]. In the chiral limit $m \rightarrow 0$, global $SU_V(3) \times SU_A(3)$ symmetry is broken down to $(U(1)_V)^2 \otimes (U(1)_A)^2$ [25]. The symmetry is even broken into $(U(1)_V)^2$, as soon as chiral symmetry is spontaneously broken.

III. SIGN PROBLEM AND CHARGE CONJUGATION OF GAUGE FIELDS

The grand canonical partition function of QCD with finite μ is obtained by

$$Z(\mu) = \int \mathcal{D}A_\mu \mathcal{D}\bar{q} \mathcal{D}q e^{-S} \quad (22)$$

with the action S of Eqs. (1)~(7) in the previous section. The path integration over the quark fields leads to

$$Z(\mu) = \int \mathcal{D}A_\mu \det[\mathcal{M}(\mu, A_\mu)] e^{-S_G}. \quad (23)$$

We start with the general case that μ and A_μ^a are complex. Using the relation

$$\begin{aligned} \mathcal{M}(\mu, A_\mu)^\dagger &= -D_\mu(A_\mu^\dagger)\gamma_\mu + m - \mu^*\gamma_4 \\ &= \gamma_5 \mathcal{M}(-\mu^*, A_\mu^\dagger) \gamma_5, \end{aligned} \quad (24)$$

one can obtain

$$\begin{aligned} \{\det[\mathcal{M}(\mu, A_\mu)]\}^* &= \det[\mathcal{M}(\mu, A_\mu)^\dagger] \\ &= \det[\gamma_5 \mathcal{M}(-\mu^*, A_\mu^\dagger) \gamma_5] \\ &= \det[\gamma_5] \det[\gamma_5] \det[\mathcal{M}(-\mu^*, A_\mu^\dagger)] \\ &= \det[\mathcal{M}(-\mu^*, A_\mu^\dagger)]. \end{aligned} \quad (25)$$

In general, the last form of (25) does not agree with $\det[\mathcal{M}(\mu, A_\mu)]$. This leads to the fact that $\det[\mathcal{M}(\mu, A_\mu)]$ is not real generally. Even in the case that μ and A_μ^a are real, Eq. (25) does not ensure that $\det[\mathcal{M}(\mu, A_\mu)]$ is real. If the integrand is not real in (25), we cannot interpret the integrand as a probability. This makes it impossible to apply the importance sampling method to the QCD action for the case of finite real μ . This is nothing but the famous sign problem.

The sign problem is originated in the fact that the fermion determinant $\det[\mathcal{M}(\mu, A_\mu)]$ is complex. For real μ and A_μ^a , however, it is always possible to make $Z(\mu)$ real by averaging the gauge configurations partially, as shown below. Using the charge conjugation matrix $C = \gamma_2\gamma_4$, one can get

$$\begin{aligned} [(C^t)^{-1} \mathcal{M}(-\mu^*, A_\mu^\dagger) C^t]^t &= D_\mu(-A_\mu^*)\gamma_\mu + m + \mu^*\gamma_4 \\ &= \mathcal{M}(\mu^*, -A_\mu^*), \end{aligned} \quad (26)$$

and, hence, [17]

$$\begin{aligned} (\det[\mathcal{M}(\mu, A_\mu)])^* &= \det[\mathcal{M}(-\mu^*, A_\mu^\dagger)] \\ &= \det(C^t)^{-1} \det[\mathcal{M}(-\mu^*, A_\mu^\dagger)] \det C^t \\ &= \det[(C^t)^{-1} \mathcal{M}(-\mu^*, A_\mu^\dagger) C^t]^t \\ &= \det[\mathcal{M}(\mu^*, -A_\mu^*)]. \end{aligned} \quad (27)$$

In QCD with real μ and A_μ^a , the relation $A_\mu^* = A_\mu^t$ leads to

$$(\det[\mathcal{M}(\mu, A_\mu)])^* = \det[\mathcal{M}(\mu, -A_\mu^t)], \quad (28)$$

where $(A_\mu^a T^a)^t = A_\mu^a T^a$ for $a = 1, 3, 4, 6, 8$ and $(A_\mu^a T^a)^t = -A_\mu^a T^a$ for $a = 2, 5, 7$. Noting the relation (28), we consider a gauge configuration $A_\mu^{a'}$ satisfying

$$A_\mu^{a'} = \sum_{a=1}^8 A_\mu^{a'} T_a = - \left(\sum_{a=1}^8 A_\mu^a T_a \right)^t = -A_\mu^t, \quad (29)$$

where $A_\mu^{a'} = -A_\mu^a$ for $a = 1, 3, 4, 6, 8$ and $A_\mu^{a'} = A_\mu^a$ for $a = 2, 5, 7$. The gauge action S_G and the Haar measure are invariant under the transformation $A_\mu \rightarrow A_\mu' = -A_\mu^t$, since this transformation is nothing but the charge conjugation for the gauge field. In fact, after this transformation, $F_{\mu\nu}$ is transformed into

$$\begin{aligned} F_{\mu\nu}' &= -\partial_\mu(A_\nu^t) + \partial_\nu(A_\mu^t) - ig[(A_\mu^t), (A_\nu^t)] \\ &= -[F_{\mu\nu}]^{\tilde{t}}, \end{aligned} \quad (30)$$

where \tilde{t} denotes the transpose operation only on the color index. Hence, the gauge action S_G is invariant under this transformation.

In QCD with real μ , we then obtain

$$\begin{aligned} (\det[\mathcal{M}(\mu, A_\mu)])^* &= \det[\mathcal{M}(\mu, -A_\mu^t)] \\ &= \det[\mathcal{M}(\mu, A_\mu')]. \end{aligned} \quad (31)$$

Averaging the integrand of $Z(\mu)$ over the two configurations A_μ and A_μ' , one can get

$$\begin{aligned} &\frac{1}{2} (\det[\mathcal{M}(\mu, A_\mu)] e^{-S_G} + \det[\mathcal{M}(\mu, A_\mu')] e^{-S_G'}) \\ &= \frac{1}{2} [\det[\mathcal{M}(\mu, A_\mu)] + (\det[\mathcal{M}(\mu, A_\mu)])^*] e^{-S_G} \\ &= \text{Re}(\det[\mathcal{M}(\mu, A_\mu)]) e^{-S_G}. \end{aligned} \quad (32)$$

This ensures that the integrand of $Z(\mu)$ becomes real.

Now we consider Z_3 -QCD. The theory tends to QCD with symmetric three flavor quarks in the $T = 0$ limit, since the difference between the two theories comes only from the temporal fermion boundary condition that has no contribution in the limit. Equation (28) is modified by the charge conjugation matrix as

$$\begin{aligned}
& \prod_{f=-1,0,1} (\det [\mathcal{M}(\mu + i2\pi f/3, A_\mu)])^* \\
&= \prod_{f=-1,0,1} \det [\mathcal{M}(\mu - i2\pi f/3, -A_\mu^t)] \\
&= \prod_{f=1,0,-1} \det [\mathcal{M}(\mu + i2\pi f/3, -A_\mu^t)] \\
&= \prod_{f=-1,0,1} \det [\mathcal{M}(\mu + i2\pi f/3, -A_\mu^t)]. \quad (33)
\end{aligned}$$

In Z_3 -QCD, the integrand of the partition function thus becomes real after the averaging procedure mentioned above. Even if the integrand of the partition function becomes real, it does not mean that the sign problem is solvable. This will be discussed later in Sec. IV.

IV. SIGN PROBLEM IN 3D 3-STATE POTTS MODEL

We first construct a Z_3 -symmetric Potts model to investigate the interplay between the sign problem and Z_3 symmetry. The standard 3D 3-state Potts model is not Z_3 -symmetric and has a sign problem, as shown below. Here we use the 3D 3-state Potts model presented in Ref. [37]. The partition function of the 3D 3-state Potts model is defined by [36,37]

$$Z(\kappa, h) = \int \mathcal{D}\Phi e^{-S} = \int \mathcal{D}\Phi e^{-S_0} e^{-S_1}; \quad (34)$$

$$S_0[\Phi_{\mathbf{x}}, \kappa] = -\kappa \sum_{\mathbf{x}, \mathbf{i}} \delta_{\Phi_{\mathbf{x}}, \Phi_{\mathbf{x}+\mathbf{i}}}, \quad (35)$$

$$S_1[\Phi_{\mathbf{x}}, h] = -\sum_{\mathbf{x}} \{h_+ \Phi_{\mathbf{x}} + h_- \Phi_{\mathbf{x}}^*\}, \quad (36)$$

$$h_+ = \exp(-\beta(M - \mu)), \quad h_- = \exp(-\beta(M + \mu)) \quad (37)$$

for the parameter κ and the unit vector \mathbf{i} in 3D space, where M and μ correspond to the mass and the chemical potential of heavy quark, respectively. In Eq. (34), $\Phi_{\mathbf{x}}$ represents a Z_3 element on site \mathbf{x} and plays a role of the Polyakov-loop operator in the Potts model, as already mentioned in Sec. I. The $\Phi_{\mathbf{x}}$ can be averaged over \mathbf{x} as

$$\bar{\Phi} = \frac{1}{V} \sum_{\mathbf{x}} \Phi_{\mathbf{x}} = \frac{1}{V} \sum_{\mathbf{x}} \Phi_{\mathbf{R},\mathbf{x}} + \frac{1}{V} \sum_{\mathbf{x}} \Phi_{\mathbf{I},\mathbf{x}} = \bar{\Phi}_{\mathbf{R}} + i\bar{\Phi}_{\mathbf{I}}, \quad (38)$$

where $\Phi_{\mathbf{x},\mathbf{R}}$ ($\bar{\Phi}_{\mathbf{R}}$) and $\Phi_{\mathbf{x},\mathbf{I}}$ ($\bar{\Phi}_{\mathbf{I}}$) mean the real and imaginary parts of $\Phi_{\mathbf{x}}$ ($\bar{\Phi}$), respectively, and V is the lattice volume. We can regard the expectation value $\langle \bar{\Phi} \rangle$ as a Polyakov loop in the Potts model, since $\langle \bar{\Phi} \rangle$ has a property similar to

the Polyakov loop $\langle L(\mathbf{x}) \rangle$ in QCD [35]. Obviously, S_0 is Z_3 -invariant, but S_1 is not. In addition, S_1 can be complex for finite μ .

In the Potts model, the sign problem is originated in the fact that the effective chemical potential is complex. If we denote the phase of $\Phi_{\mathbf{x}}$ as $\phi_{\mathbf{x}}$, Eq. (36) is rewritten as

$$S_1[\Phi_{\mathbf{x}}, h] = -2e^{-\beta M} \sum_{\mathbf{x}} |\Phi_{\mathbf{x}}| \cosh(\beta \tilde{\mu}_{\mathbf{x}}) \quad (39)$$

with the complex effective chemical potential $\beta \tilde{\mu}_{\mathbf{x}} = \beta \mu + i\phi_{\mathbf{x}}$. When $\tilde{\mu}_{\mathbf{x}}$ is complex, it makes $\cosh(\beta \tilde{\mu}_{\mathbf{x}})$ complex in S_1 and consequently induces the sign problem. In this sense, the entanglement between μ and $i\phi_{\mathbf{x}}$ is an origin of the sign problem in the Potts model. When μ is pure imaginary, so is $\tilde{\mu}$: namely $S_1^* = S_1$. This make the model free from the sign problem.

The Potts model is constructed by simplifying the heavy-dense model of QCD in the limit of $M \rightarrow \infty$ and $\mu \rightarrow \infty$ with $M - \mu$ fixed at a finite value. Therefore, the Potts model should be considered for large M and μ . The term having h_- is occasionally neglected, but is retained in the present paper.

In the Potts model, Z_3 elements are taken as three states at each site on a 3D lattice. Considering the Z_3 elements as a substitute for the Polyakov-loop operator $L(\mathbf{x})$ in QCD, one can discuss the deconfinement transition through the 3D Potts model. The operator $L(\mathbf{x})$ depends on both \mathbf{x} and T , but information on T is eliminated in the Potts model as a result of the substitution. Furthermore, in the 3D Potts model, there is no temporal direction and the average over spatial volume should be taken on the Polyakov loop. However, the Potts model has a parameter κ in S_0 . It was found in Ref. [35] that κ dependence of $\langle \bar{\Phi} \rangle$ in the Potts model is similar to T dependence of $\langle L(\mathbf{x}) \rangle$ in QCD. Although the relation between κ and T is not simple, we assume that larger (smaller) κ in the Potts model corresponds to higher (lower) T in QCD and $1/\beta$ is just a parameter having the same dimension as M and μ . Below, we mainly use dimensionless parameters $\hat{M} = \beta M$ and $\hat{\mu} = \beta \mu$ instead of dimensionful ones M and μ .

The factor e^{-S_1} in (34) can be rewritten as $e^{-iS_1 - S_{\mathbf{R}}}$ with

$$S_{\mathbf{R}}[\Phi_{\mathbf{x}}, \hat{M}, \hat{\mu}] = -2e^{-\hat{M}} \cosh(\hat{\mu}) V \bar{\Phi}_{\mathbf{R}}, \quad (40)$$

$$S_{\mathbf{I}}[\Phi_{\mathbf{x}}, \hat{M}, \hat{\mu}] = -2e^{-\hat{M}} \sinh(\hat{\mu}) V \bar{\Phi}_{\mathbf{I}}. \quad (41)$$

Since $\Phi_{\mathbf{x}}$ takes any value of Z_3 elements, $e^{i2\pi k/3}$ ($k = -1, 0, 1$), S_1 becomes complex in general when $\mu \neq 0$. Hence, we take the configuration average over $\Phi_{\mathbf{x}}$ and $\Phi_{\mathbf{x}}' = \Phi_{\mathbf{x}}^*$, following the discussion in the previous section:

$$\begin{aligned} & \frac{1}{2} \{ e^{(-S_0[\Phi_x, \kappa])} e^{(-S_1[\Phi_x, h])} + e^{(-S_0[\Phi'_x, \kappa])} e^{(-S_1[\Phi'_x, h])} \} \\ & = \cos(S_1[\Phi_{x,I}, \hat{M}, \hat{\mu}]) e^{(-S_0[\Phi_x, \kappa] - S_R[\Phi_{x,R}, \hat{M}, \hat{\mu}])}. \end{aligned} \quad (42)$$

The integrand of the partition function (34) thus becomes real, but the cosine function becomes negative when

$$\frac{\pi}{2} \leq 2e^{-\hat{M}} \sinh(\hat{\mu}) V \Phi_1 \leq \frac{3\pi}{2} \pmod{[2\pi]}. \quad (43)$$

Hence, the sign problem appears even after the averaging procedure and it becomes stronger as V increases.

It is known that, although the Potts model has a sign problem in its path integral formulation, the model can be transformed into a “flux model” that has no complex action problem [18,19]. However, it is not clear that such a transformation is possible or not in the case of full LQCD simulations. Since we are interested in the sign problem itself, we treat the 3D Potts model in the formulation where the sign problem is obvious.

Since the 3D 3-state Potts model has a sign problem in our formulation, namely, $F(\Phi_x) = e^{-S}$, it becomes complex in general. Hence, we consider the following phase quenched approximation:

$$\langle O \rangle' = \frac{\int \mathcal{D}\Phi O(\Phi_x) F'(\Phi_x)}{Z'}; \quad (44)$$

$$\begin{aligned} F'(\Phi_x) &= e^{-S_0 - S_R}, \\ Z' &= \int \mathcal{D}\Phi F'(\Phi_x). \end{aligned} \quad (45)$$

The phase factor $\langle F/F' \rangle$ and the true average $\langle O \rangle$ are then given by

$$\begin{aligned} \left\langle \frac{F}{F'} \right\rangle' &= \langle e^{-iS_1} \rangle' = \frac{\int \mathcal{D}\Phi [e^{-iS_1}] F'(\Phi_x)}{Z'} \\ &= \frac{\int \mathcal{D}\Phi [\cos S_1] F'(\Phi_x)}{Z'} = \langle \cos S_1 \rangle' = \frac{Z}{Z'}, \end{aligned} \quad (46)$$

$$\langle O \rangle = \frac{\int \mathcal{D}\Phi [O] F(\Phi_x)}{Z} = \frac{\langle O(\Phi_x) e^{-iS_1} \rangle'}{\langle \frac{F}{F'} \rangle'}. \quad (47)$$

Since Φ_x can be complex in general, the calculation of the expectation value of the Polyakov loop itself is somewhat complicated when the sign problem appears. Hence, for convenience, we calculate the absolute value $|\bar{\Phi}|$ instead of $\bar{\Phi}$ itself by using Monte Carlo simulations. To calculate physical quantities in a wide region of κ - μ plane, we took a rather small lattice with spatial volume $V = 6^3$. For this reason, in this paper we postpone the determination of the order of the deconfinement transition and simply define the

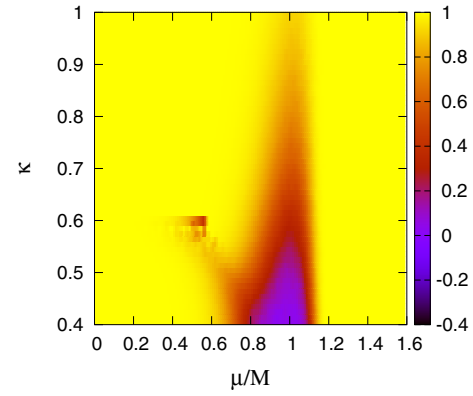


FIG. 1. The phase factor $\langle \cos S_1 \rangle'$ calculated with the phase quenched approximation in ordinary 3D 3-state Potts model as a function of κ and μ/M .

transition point with the point where $\langle \bar{\Phi} \rangle \sim 0.5$. We also put $\hat{M} = 10$ below.

Figure 1 shows the results of the phase factor $\langle \cos S_1 \rangle'$ calculated with the quenched approximation in the κ - μ plane. The sign problem is serious in a “triangle” area composed of three points $(\mu/M, \kappa) \approx (0.8, 0.4)$, $(1.1, 0.4)$, $(1, 0.6)$, since $\langle \cos S_1 \rangle'$ is small or negative there.

Figure 2 shows the results of $\langle |\bar{\Phi}| \rangle$ calculated with the reweighting method in the κ - μ plane. The line where $\langle |\bar{\Phi}| \rangle$ rapidly changes can be regarded as a “critical line” $\kappa = \kappa_c(\mu/M)$. The value of $\kappa_c(\mu/M)$ is about 0.55 for $\mu/M < 0.5$, but rapidly decreases from 0.55 to 0.4 as μ/M increases from 0.5 to 0.75.

Comparing Fig. 1 with Fig. 2, we can see, as an interesting property, that $\langle \cos S_1 \rangle'$ tends to be small on the critical line particularly in $0.4 < \mu/M < 0.75$. In the triangle area composed of three points $(\mu/M, \kappa) \approx (0.8, 0.4)$, $(1.1, 0.4)$, $(1, 0.6)$, the value of $\langle |\bar{\Phi}| \rangle$ is larger than 1 or negative, since $\langle \cos S_1 \rangle'$ is small or negative. The unnatural

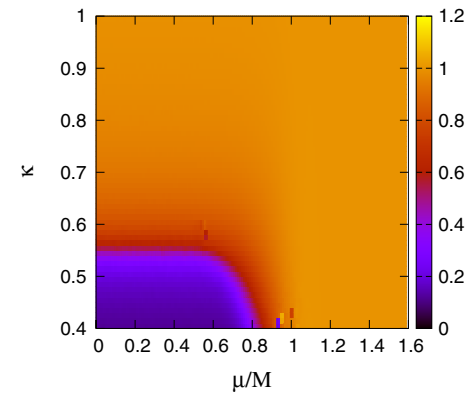


FIG. 2. The expectation value $\langle |\bar{\Phi}| \rangle$ calculated with the reweighting method in ordinary 3D 3-state Potts model as a function of κ and μ/M .

behavior of $\langle |\bar{\Phi}| \rangle$ is caused by that of $\langle \cos S_1 \rangle'$. Therefore, physical discussion cannot be made in the triangle region.

V. Z_3 -SYMMETRIC 3D POTTS MODEL

Using the same method as the extension of QCD to Z_3 -QCD, we now construct a Z_3 -symmetric 3D Potts model from the 3D Potts model defined in the previous section. The action S_{Z_3} of the new model is assumed to be described in a power series of Φ_x and Φ_x^* just as the original Potts model, and the flavor-dependent imaginary chemical potentials are introduced by replacing $h_+ \Phi_x$, $h_- \Phi_x^*$ by

$$h_{+,f} \Phi_x = e^{i2\pi f/3} \exp(\hat{\mu} - \hat{M}) \Phi_x, \quad (48)$$

$$h_{-,f} \Phi_x^* = e^{-i2\pi f/3} \exp(-\hat{\mu} - \hat{M}) \Phi_x^*. \quad (49)$$

Here we consider Z_3 elements as three states of Φ_x for a while, but will increase the number of states later in which some states do not belong to the group Z_3 .

The pure gauge and first-order terms, S_{0,Z_3} and S_{1,Z_3} , of S_{Z_3} are then defined as

$$S_{0,Z_3}[\Phi_x, \kappa] = -\kappa \sum_{x,i} |\Phi_x| |\Phi_{x+i}| \delta_{\Phi_x, \Phi_{x+i}}, \quad (50)$$

$$S_{1,Z_3}[\Phi_x, h_{\pm}] = - \sum_{f=-1,0,1} \sum_x (h_{+,f} \Phi_x + h_{-,f} \Phi_x^*). \quad (51)$$

Here, S_{0,Z_3} is Z_3 invariant, but S_{1,Z_3} is Z_3 variant. Note that S_{0,Z_3} is reduced to S_0 when the values of Φ_x are restricted to

$$\begin{aligned} & \sum_{f=-1,0,1} \log(1 + 3h_{+,f} \Phi_x + 3h_{+,f}^2 \Phi_x^* + (h_{+,f})^3) + \sum_{f=-1,0,1} \log(1 + 3h_{-,f} \Phi_x^* + 3h_{-,f}^2 \Phi_x + (h_{-,f})^3) \\ &= \log \left[\prod_{f=-1,0,1} (1 + 3h_{+,f} \Phi_x + 3h_{+,f}^2 \Phi_x^* + (h_{+,f})^3) \right] + \log \left[\prod_{f=-1,0,1} (1 + 3h_{-,f} \Phi_x^* + 3h_{-,f}^2 \Phi_x + (h_{-,f})^3) \right] \\ &= \log[(a + 27(h_+)^3 \Phi_x^3 + 27(h_+)^6 \Phi_x^{*3} + \dots)] + \log[(b + 27(h_-)^3 \Phi_x^3 + 27(h_-)^6 \Phi_x^{*3} + \dots)], \end{aligned} \quad (57)$$

where a and b are Φ_x -independent real quantities. On the other hand, the terms proportional to $\Phi_x \Phi_x^*$ are expected to appear if the mesonic contribution in the effective Lagrangian is expanded.

The factor $e^{-S_{2+3,Z_3}}$ can be rewritten into

$$e^{-S_{2,Z_3} - S_{3,Z_3}} = e^{-iS_{1,Z_3}} e^{-S_{R,Z_3}} e^{-S_{2,Z_3}} \quad (58)$$

with

$$S_{R,Z_3}[\Phi_x, \hat{M}, \hat{\mu}] = -2e^{-3\hat{M}} \cosh(3\hat{\mu}) \sum_x (\Phi_x^3)_R, \quad (59)$$

Z_3 elements only. If the f summation is taken in S_{1,Z_3} , the term vanishes as follows:

$$\begin{aligned} S_{1,Z_3}[\Phi_x, h_{\pm}] &= - \sum_{f=-1,0,1} \sum_x (h_{+,f} \Phi_x + h_{-,f} \Phi_x^*) \\ &= \sum_x (h_+ \Phi_x + h_- \Phi_x^*) \sum_{f=-1,0,1} e^{i2\pi f/3} = 0. \end{aligned} \quad (52)$$

Similarly, any Z_3 -variant terms vanish after the f summation. Considering the power series of S_{Z_3} up to the third order of Φ_x and Φ_x^* , we can construct a Z_3 -symmetric Potts model as

$$Z(\kappa, h_M, h_{\pm}) = \int \mathcal{D}\Phi e^{-S_{Z_3}} = \int \mathcal{D}\Phi e^{-S_{0,Z_3}} e^{-S_{2+3,Z_3}}, \quad (53)$$

where $h_M = e^{-\hat{M}}$ and

$$S_{2+3,Z_3}[\Phi_x, h_M, h_{\pm}] = S_{2,Z_3}[\Phi_x, h_M] + S_{3,Z_3}[\Phi_x, h_{\pm}]; \quad (54)$$

$$S_{2,Z_3}[\Phi_x, h_M] = -g_2 h_M^2 \sum_x \Phi_x \Phi_x^*, \quad (55)$$

$$S_{3,Z_3}[\Phi_x, h_{\pm}] = -g_3 \sum_x (h_+^3 \Phi_x^3 + h_-^3 \Phi_x^{*3}) \quad (56)$$

with the coupling parameters g_2 and g_3 . For simplicity, we take $g_2 = g_3 = 1$. Note that, e.g., the third-order terms of Φ_x can appear when the logarithmic Fermionic effective Lagrangian [13] is expanded by Φ_x as

$$S_{1,Z_3}[\Phi_x, \hat{M}, \hat{\mu}] = -2e^{-3\hat{M}} \sinh(3\hat{\mu}) \sum_x (\Phi_x^3)_I \quad (60)$$

for the real and imaginary parts, $(\Phi_x^3)_R$ and $(\Phi_x^3)_I$, of Φ_x^3 . When the values of Φ_x are restricted to Z_3 elements, both S_{0,Z_3} and S_{2+3,Z_3} are real, indicating that no sign problem takes place. This model is referred to as the “ Z_3 -symmetric 3-state Potts model” in the present paper.

Meanwhile, the Z_3 -symmetric heavy-dense model of QCD has the sign problem, since the Polyakov-loop

operator $L(\mathbf{x})$ can take not only Z_3 elements but also ones not belonging to the group Z_3 . In the model, $L(\mathbf{x})$ can be parametrized as [13]

$$L(\mathbf{x}) = \frac{1}{3}(e^{i\phi_1(\mathbf{x})} + e^{i\phi_2(\mathbf{x})} + e^{-i(\phi_1(\mathbf{x})+\phi_2(\mathbf{x}))}), \quad (61)$$

and the region that $L(\mathbf{x})$ can take is illustrated in Fig. 3(a). The region has a hyperbolic-triangle-like shape. Three vertices of the triangle correspond to Z_3 elements, and the other points in the region do not belong to the group Z_3 . Figure 3(b) corresponds to the region that $L^3(\mathbf{x})$ is allowed to take. The allowed region of $L^3(\mathbf{x})$ is well localized near the real axis compared with that of $L(\mathbf{x})$. This suggests that the sign problem is less serious in Z_3 -QCD than in QCD [27]. Since it is not easy to confirm this suggestion directly in QCD, we will compare three types of models: (i) the original Potts model, (ii) the Z_3 -symmetric 3-state Potts model defined above, and (iii) the Z_3 -symmetric *several-state* Potts models, each with different number of states larger than 3. The Z_3 -symmetric several-state Potts model is an extension of the Z_3 -symmetric 3-state Potts model and is not free from the sign problem in general.

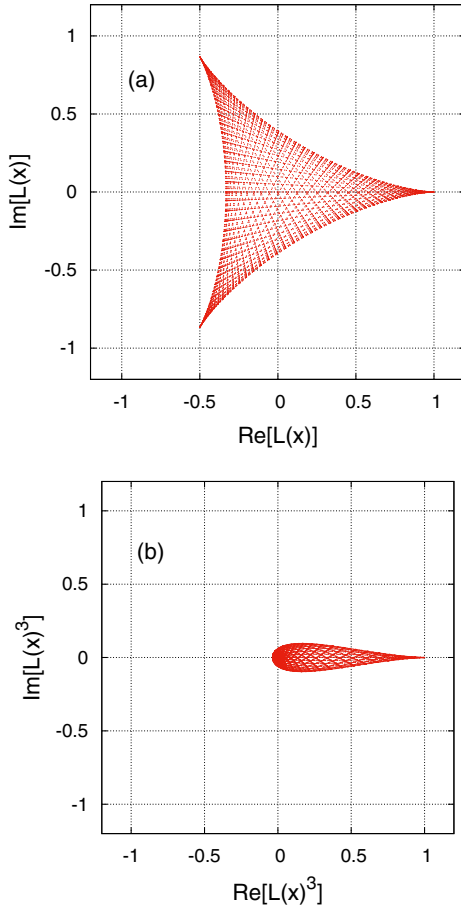


FIG. 3. Allowed regions of (a) $L(\mathbf{x})$ and (b) $L^3(\mathbf{x})$ in the complex plane.

Before constructing Z_3 -symmetric several-state Potts models explicitly, we make the following preparation. When the $\Phi_{\mathbf{x}}$ are allowed to take values not belonging to the group Z_3 just as the heavy quark model, the term S_{2+3,Z_3} can be complex. In that case, we take the average of $\Phi_{\mathbf{x}}$ and $\Phi'_{\mathbf{x}} = \Phi_{\mathbf{x}}^*$ configurations to make the partition function real, following the discussion in the previous section. This leads to

$$\frac{e^{-S_{0,Z_3}[\Phi_{\mathbf{x}}]} e^{-S_{2+3,Z_3}[\Phi_{\mathbf{x}}]} + e^{-S_{0,Z_3}[\Phi'_{\mathbf{x}}]} e^{-S_{2+3,Z_3}[\Phi'_{\mathbf{x}}]}}{2} = \cos(S_{I,Z_3}[\Phi_{\mathbf{x}}]) e^{(-S_{0,Z_3}[\Phi_{\mathbf{x}}] - S_{2,Z_3}[\Phi_{\mathbf{x}}] - S_{R,Z_3}[\Phi_{\mathbf{x}}])}. \quad (62)$$

The integrand of the partition function (53) thus becomes real, but the cosine function becomes negative when

$$\frac{\pi}{2} \leq 2e^{-3\hat{M}} \sinh(3\hat{\mu}) \sum_{\mathbf{x}} (\Phi_{\mathbf{x}}^3)_I \leq \frac{3\pi}{2} \pmod{[2\pi]}. \quad (63)$$

As mentioned in Fig. 3, however, the absolute value of the imaginary part $\text{Im}[L(\mathbf{x})^3]$ is much smaller than that of $\text{Im}[L(\mathbf{x})]$. This is true also in the Z_3 -symmetric Potts models with several states; namely, $\max[|(\Phi_{\mathbf{x}}^3)_I|] \ll \max[|(\Phi_{\mathbf{x}})_I|]$. Hence, it can be expected that the sign problem is less serious in the Z_3 -symmetric Potts model with several states than in the original Potts model without exact Z_3 symmetry.

Now we explicitly consider four kinds of Z_3 -symmetric Potts models, each with 3, 4, 7, and 13 states:

(A) Z_3 -symmetric 3D 3-state Potts model with

$$\{\Phi_{\mathbf{x}}\} = \{1, e^{\pm i2\pi/3}\}, \quad (64)$$

which is denoted by three solid triangle symbols in Fig. 4. This model is free from the sign problem, since S_{2+3,Z_3} is always real.

(B) Z_3 -symmetric 3D 4-state Potts model with

$$\{\Phi_{\mathbf{x}}\} = \{1, e^{\pm i2\pi/3}, 0\}, \quad (65)$$

which is denoted by three solid triangles and a solid circle in Fig. 4. The sign problem does not appear.

(C) Z_3 -symmetric 3D 7-state Potts model with

$$\{\Phi_{\mathbf{x}}\} = \{1, e^{\pm i2\pi/3}, 0, -1/3, e^{\pm i\pi/3}/3\}, \quad (66)$$

which is denoted by three solid triangles, a solid circle and three solid squares in Fig. 4. The sign problem does not appear.

(D) Z_3 -symmetric 3D 13-state Potts model with

$$\{\Phi_{\mathbf{x}}\} = \{1, e^{\pm i2\pi/3}, 0, -1/3, e^{\pm i\pi/3}/3, re^{\pm i\pi/6}, re^{\pm i\pi/2}, re^{\pm i5\pi/6}\}, \quad (67)$$

where r is taken to be 0.4. Equation (67) is denoted by three solid triangles, a solid circle, three

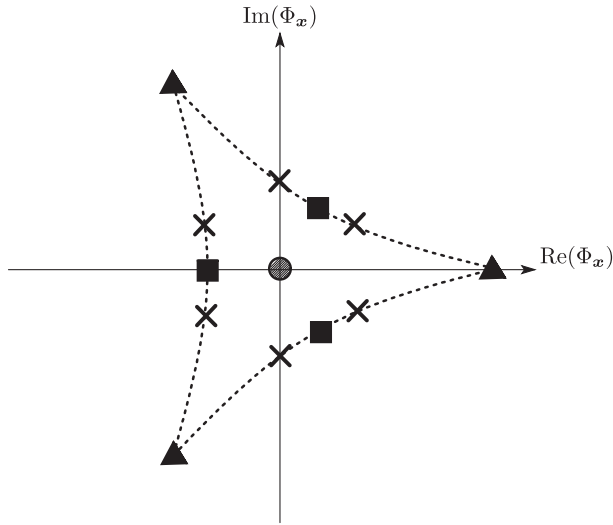


FIG. 4. Values of Φ_x taken in the Z_3 -symmetric 3D Potts models (A)–(D).

solid squares and six crosses in Fig. 4. Note that, except for the origin, the other 12 values are chosen to lie on the boundary of the region where the value of $L(x)$ can be taken in Fig. 3(a). The sign problem comes from six crosses $\{\Phi_x\} = \{re^{\pm i\pi/6}, re^{\pm i\pi/2}, re^{\pm i5\pi/6}\}$, since $(\Phi_x)^3$ has a finite phase in this case.

Properties of the four Z_3 -symmetric Potts models (A)–(D) are summarized in Table I, together with those of the original 3D 3-state Potts model.

Before closing this section, we add one more comment. If we denote $\Phi_x = r_x \exp(i\phi_x)$, where r_x and ϕ_x are the absolute value and the phase of Φ_x , respectively, $(\Phi_x)^3 = r_x^3 \exp(3i\phi_x) = r_x^3 (\cos(3\phi_x) + i \sin(3\phi_x))$. Therefore, if r_x is small, the sign problem is not severe. Hence, it can be expected that, for fixed ϕ_x , larger r_x configurations dominate the sign problem. So we choose our simulation points on the boundary of the hyperbolic triangle in Fig. 4, except for the origin, the special point for confinement. Furthermore, to keep the Z_3 symmetry, we use the configurations of Φ_x with the discrete phase $\phi_x^j = 2\pi j/(3n)$ ($j = 0, 1, 2, \dots, n-1$), where n is a positive integer. In principle, the calculation is possible by using the other points on the boundary with larger $n > 4$, but it requires huge computing time. Estimation of the contributions of other points is an open question for the future.

VI. SIGN PROBLEM IN Z_3 -SYMMETRIC POTTS MODEL

In this section, we perform numerical simulations for the Z_3 -symmetric Potts models (A)–(D) and compare the results with those of the original Potts model. In particular, the expectation value $\langle |\bar{\Phi}| \rangle$ of the absolute value $|\bar{\Phi}|$ is calculated to determine the confinement-deconfinement

transition line. The purpose of these analyses is to (1) clarify the interplay between Z_3 symmetry and the sign problem and (2) see how the deconfinement transition line changes in the κ - μ plane when the value of Φ_x is extended bit by bit. As mentioned in Sec. IV, the standard Metropolis algorithm is taken for the simulations.

A. Z_3 -symmetric 3D 3-state Potts model

Figure 5 shows the expectation value $\langle |\bar{\Phi}| \rangle$ in the κ - μ plane for model (A). Note that the reweighting is not necessary for this model, since the model has no sign problem. There appears a rapid change of $\langle |\bar{\Phi}| \rangle$ at $\kappa = 0.55$, independently of μ . The μ independence comes from the fact that the μ -dependent term S_{2+3, Z_3} becomes constant because of $\Phi_x(\Phi_x)^* = \Phi_x^3 = \Phi_x^{*3} = 1$. In fact, $\langle |\bar{\Phi}| \rangle$ can be rewritten as

$$\begin{aligned} \langle |\bar{\Phi}| \rangle &= \frac{\int \mathcal{D}\Phi |\bar{\Phi}| e^{-S_{0, Z_3} - S_{2+3, Z_3}}}{\int \mathcal{D}\Phi e^{-S_{0, Z_3} - S_{2+3, Z_3}}} \\ &= \frac{e^{-S_{2+3, Z_3}} \int \mathcal{D}\Phi |\bar{\Phi}| e^{-S_{0, Z_3}}}{e^{-S_{2+3, Z_3}} \int \mathcal{D}\Phi e^{-S_{0, Z_3}}} \\ &= \frac{\int \mathcal{D}\Phi |\bar{\Phi}| e^{-S_{0, Z_3}}}{\int \mathcal{D}\Phi e^{-S_{0, Z_3}}}. \end{aligned} \quad (68)$$

The final form of Eq. (68) has no μ dependence. However, this does not mean that all quantities do not depend on μ . In fact, the number density,

$$\begin{aligned} n &= \frac{1}{\beta V} \frac{\partial(\log Z)}{\partial \mu} = \frac{1}{V} \frac{\partial(\log Z)}{\partial \hat{\mu}} \\ &= \frac{6e^{-3\hat{M}}}{V} \left[\sinh(3\hat{\mu}) \left\langle \sum_x (\Phi_x^3)_R \right\rangle \right. \\ &\quad \left. + i \cosh(3\hat{\mu}) \left\langle \sum_x (\Phi_x^3)_I \right\rangle \right], \end{aligned} \quad (69)$$

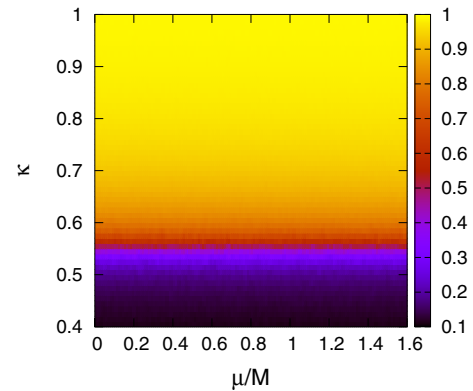


FIG. 5. The expectation value $\langle |\bar{\Phi}| \rangle$ in the Z_3 -symmetric 3D 3-state Potts model as a function of κ and μ/M .

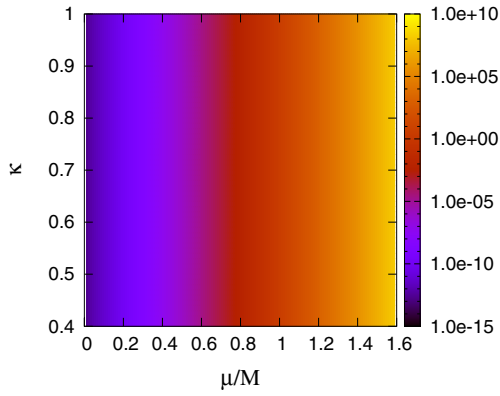


FIG. 6. The expectation value n in the Z_3 -symmetric 3D 3-state Potts model as a function of κ and μ/M . Note that n is dimensionless, since the dimensionless volume $V = 6^3$ is used in calculations of (69).

has μ dependence, as shown in Fig. 6. (Note that (68) is true only in the 3D 3-state Z_3 -symmetric Potts model, whereas (69) is true for all Z_3 -symmetric Potts models.) The quark number density n can be regarded as an order parameter for the onset phase transition that is located at $\mu/M = 1$ and $T = 0$. Below we will see how the two transitions entangle each other and the sign problem appears when the value region of Φ_x is extended bit by bit. Note that the second term in the second line of (69) vanishes when $(\Phi_x^3)_I = 0$ and the sign problem does not appear.

In Fig. 7, the μ -dependence of n is shown at $\kappa = 0.65$ for three Z_3 -symmetric Potts models. When $\kappa = 0.65$, in the Z_3 -symmetric 3-state Potts model, the onset of n is smooth and n is proportional to $e^{-3\hat{M}} \sinh 3\hat{\mu}$ in the model, since $(\Phi_x^3)_R = 1$ and $(\Phi_x^3)_I = 0$ in (69).

It is interesting that, in the Z_3 -symmetric 3D 3-s Potts model, the resulting deconfinement transition line then becomes a horizontal line in the μ - κ plane. Similar property

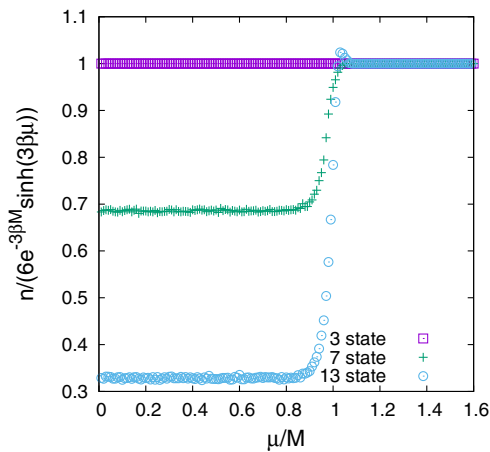


FIG. 7. μ -dependence of n at $\kappa = 0.65$ in the Z_3 -symmetric 3D Potts model. The boxes, the crosses, and the circles represent the results in 3-, 7-, and 13-state Potts models.

is also seen in $SU(N)$ gauge theory in the large N limit [41,42], where the contribution of the fermion with N degrees of freedom to the thermodynamic potential is negligible compared with that of gauge field with $N^2 - 1$ degrees of freedom. In the case of Z_3 -symmetric theory, Z_3 symmetry suppresses the fermion contribution and weakens the μ dependence of the critical temperature of the deconfinement transition [24].

B. Z_3 -symmetric 3D 4-state Potts model

In this case, the model has no sign problem as is in the previous one. Figure 8 shows the expectation value $\langle |\bar{\Phi}| \rangle$ in the κ - μ plane. The deconfinement transition line $\kappa = \kappa_c(\mu/M)$ defined by a rapid change of $\langle |\bar{\Phi}| \rangle$ is located at $\kappa = 0.60$ for $\mu/M < 1$, but goes down to $\kappa = 0.55$ at $\mu/M \approx 1$, and keeps $\kappa = 0.55$ for $\mu/M > 1$.

Thus, the deconfinement transition is beginning to have μ dependence.

C. Z_3 -symmetric 3D 7-state Potts model

In this case, the model has no sign problem as is in the previous two cases. Figure 9 shows the expectation value $\langle |\bar{\Phi}| \rangle$ in the κ - μ plane. The deconfinement transition line $\kappa = \kappa_c(\mu/M)$ is located at $\kappa = 0.7$ for $\mu/M < 1$, but goes down to $\kappa = 0.55$ at $\mu/M \approx 1$, and keeps $\kappa = 0.55$ for $\mu/M > 1$. The deconfinement transition line thus has stronger μ dependence in model (C) than in model (B). Figure 10 shows μ dependence of $\langle |\bar{\Phi}| \rangle$ with κ fixed at 0.65. We can see that $\langle |\bar{\Phi}| \rangle$ suddenly increases at $\mu/M \approx 1$. In Fig. 7, the μ dependence of n is shown. In this model, n also rapidly increases at $\mu/M \approx 1$.

D. Z_3 -symmetric 3D 13-state Potts model

In model (D), when S_{2+3,Z_3} becomes complex, $F(\Phi_x) = e^{-S}$ also does, so that the sign problem appears. We then use the following phase quenched approximation:

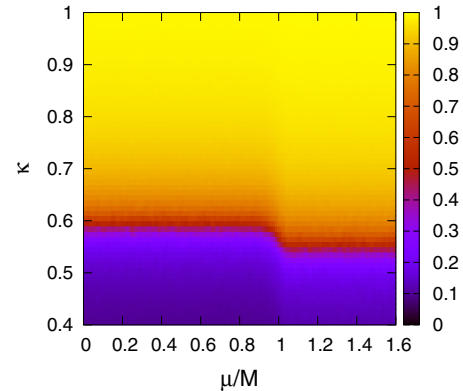


FIG. 8. The expectation value $\langle |\bar{\Phi}| \rangle$ in the Z_3 -symmetric 3D 4-state Potts model as a function of κ and μ/M .

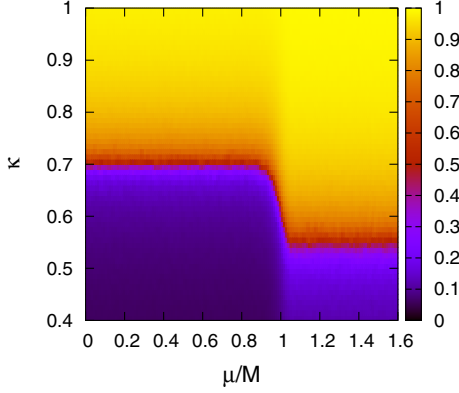


FIG. 9. The expectation value $\langle |\bar{\Phi}| \rangle$ in Z_3 -symmetric 3D 7-state Potts model as a function of κ and μ/M .

$$\langle O \rangle' = \frac{\int \mathcal{D}\Phi O(\Phi_x) F'(\Phi_x)}{Z'}; \quad (70)$$

$$F'(\Phi_x) = e^{-S_{0,Z_3} - S_{2,Z_3} - S_{R,Z_3}},$$

$$Z' = \int \mathcal{D}\Phi F'(\Phi_x). \quad (71)$$

The phase factor is then given by

$$\left\langle \frac{F}{F'} \right\rangle' = \langle e^{-iS_{1,Z_3}} \rangle' = \frac{\int \mathcal{D}\Phi [e^{-iS_{1,Z_3}}] F'(\Phi_x)}{Z'}$$

$$= \frac{\int \mathcal{D}\Phi [\cos S_{1,Z_3}] F'(\Phi_x)}{Z'} = \langle \cos S_{1,Z_3} \rangle' = \frac{Z}{Z'}, \quad (72)$$

and the true average $\langle O \rangle$ is by

$$\langle O \rangle = \frac{\int \mathcal{D}\Phi [O] F'(\Phi_x)}{Z} = \frac{\langle O(\Phi) e^{-iS_{1,Z_3}} \rangle'}{\langle \frac{F}{F'} \rangle'}. \quad (73)$$

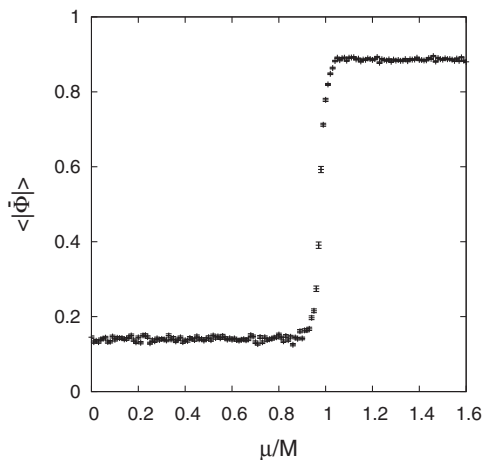


FIG. 10. μ -dependence of $\langle |\bar{\Phi}| \rangle$ at $\kappa = 0.65$ in the Z_3 -symmetric 3D 7-state Potts model.

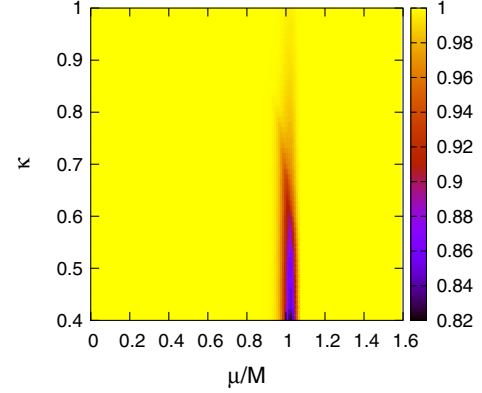


FIG. 11. The expectation value $\langle \cos S_{1,Z_3} \rangle'$ calculated with the phase quenched approximation in the Z_3 -symmetric 3D 13-state Potts model as a function of κ and μ/M .

Figure 11 shows the phase factor (72) in the κ - μ plane. As an important result, the sign problem is serious only in the narrow region of $\mu/M \sim 1$ and $\kappa < 0.9$.

Figure 12 shows the expectation value of $\langle |\bar{\Phi}| \rangle$ in the κ - μ plane. The result was obtained by using the quenched approximated probability function and the reweighting method. The deconfinement transition line $\kappa = \kappa_c(\mu/M)$ is located at $\kappa = 0.87$ for $\mu/M < 1$, but goes down to $\kappa = 0.55$ at $\mu/M \approx 1$, and keeps $\kappa = 0.55$ for $\mu/M > 1$. Thus, the μ dependence of $\kappa = \kappa_c(\mu/M)$ becomes strong as the number of states on each site increases. Eventually, the transition line of model (D) is rather similar to that of the original Potts model. Nevertheless, as for the seriousness of the sign problem, there is a big difference between the two models. Comparing Fig. 11 with Fig. 1, we can conclude that the sign problem is almost cured by Z_3 symmetry, even if the value region of Φ_x is extended.

It is interesting that, in Fig. 11, the narrow dark region (where the phase factor is small) lies on the line $\mu/M \approx 1$ where the onset transition takes place. In fact, as shown in Fig. 7, n rapidly increases at $\mu/M \approx 1$. Of course, this dark region may be only an artifact due to the sign problem, but

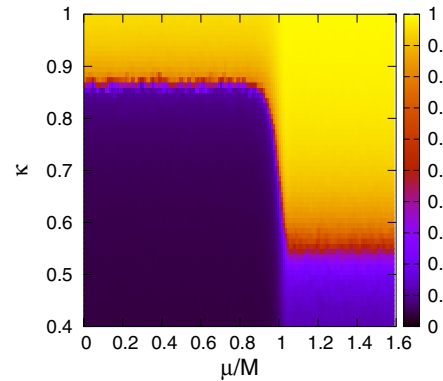


FIG. 12. The expectation value $\langle |\bar{\Phi}| \rangle$ calculated with the reweighting method in Z_3 -symmetric 3D 13-state Potts model as a function of κ and μ/M .

may imply that a physical sharp transition occurs on the line and the partition function $Z(\mu)$ becomes small around the line. Hence, Lee-Yang zeros analyses [43] may be valid in this phenomena. On the contrary, the deconfinement transition appears on the line of $\kappa \sim 0.87$ and $\mu/M < 1$ in Fig. 12, but any dark area is not found around the line in Fig. 11. This may be caused by the fact that the lattice size is small in our simulations and the deconfinement transition does not induce any singular behavior in the partition function. This is an interesting question to be solved in future.

VII. SUMMARY

In summary, we have constructed four versions of the Z_3 -symmetric 3D Potts models, each with a different number of states, in order to investigate (1) the interplay between Z_3 symmetry and the sign problem and (2) the relation between the number of states and the deconfinement transition line in the μ - κ plane. Properties of the four Z_3 -symmetric Potts models (A)–(D) are summarized in Table I, together with those of the original 3D 3-state Potts model.

As for subject (1), we have found from the comparison between the Potts model and model (D) that the sign problem is almost cured by imposing Z_3 symmetry. The Z_3 -symmetric Potts models are described by a power series of the Polyakov-loop operator Φ_x and its complex conjugate Φ_x^* . Z_3 symmetry eliminates the linear term, so that the imaginary part of the model action starts with the terms of $(\Phi_x)^3$ and $(\Phi_x^*)^3$. This makes the sign problem less serious, because of $|\Phi_x| < 1$; note that only Z_3 elements satisfy $|\Phi_x| = 1$, but they do not contribute to the imaginary part. This mechanism may happen in Z_3 -QCD. Therefore, there is a possibility that the sign problem is circumvented by the Taylor-expansion method of Ref. [27] to derive QCD results from Z_3 -QCD ones, even if $T \neq 0$.

Subject (2) was clarified by changing the number of states from 3 of model (A) to 13 of model (D). Comparing the results of model (A)–(D), we have found that the μ dependence of the deconfinement transition line becomes stronger with respect to increasing the number of states.

The lattice size we used is not enough, so that there is a possibility that the sign problem becomes more serious as the lattice volume becomes larger. We also postponed the determination of the order of the deconfinement transition for the same reason. The study based on larger lattice is needed as a future work.

There is a possibility that, as in the original Potts model [18], the Z_3 symmetric Potts model also can be transformed into the flux model that has no sign problem. In Ref. [19], the effective model based on the Polyakov loop, the values of which are not restricted to Z_3 element, was transformed into the flux model. However, except for pure gauge term, only the linear terms of Φ_x are considered in that formalism. The extension of the formalism to the Z_3 -symmetric Potts model is nontrivial, because the extension to the case with higher Φ_x terms is nontrivial. Therefore, we postpone the extension for a future work.

In the Potts models, chiral symmetry and its dynamical breaking cannot be discussed, since these models consider the case of large quark mass, and thereby chiral symmetry is largely broken from the beginning. In QCD with light quark masses, when the phase quenched approximation is used, chiral dynamics induces the problem of early onset of quark number density [44] (or the baryon Silver Blaze problem [45]). The problem may happen also in Z_3 -QCD with light quark masses. Analyses beyond the phase quenched approximation may be important for future work.

ACKNOWLEDGMENTS

The authors are thankful especially to Hiroshi Suzuki and Hiroshi Yoneyama for crucial discussions on the realization of the QCD partition function. The authors also thank Atsushi Nakamura, Etsuko Itou, Masahiro Ishii, Junpei Sugano, Akihisa Miyahara, Shuichi Togawa, and Yuhei Torigoe for fruitful discussions. H. K. also thanks Motoi Tachibana, Tatsuhiko Misumi, Yuya Tanizaki, and Kouji Kashiwa for useful discussions. H. K. and M. Y. are supported by Grants-in-Aid for Scientific Research (No. 26400279 and No. 26400278) from the Japan Society for the Promotion of Science (JSPS). The numerical calculations were partially performed by using SX-ACE at CMC, Osaka University.

[1] Z. Fodor and S. D. Katz, *Phys. Lett. B* **534**, 87 (2002).
 [2] P. de Forcrand and O. Philipsen, *Nucl. Phys.* **B642**, 290 (2002).
 [3] M. D’Elia and M. P. Lombardo, *Phys. Rev. D* **67**, 014505 (2003).
 [4] M. D’Elia and F. Sanfilippo, *Phys. Rev. D* **80**, 111501 (2009).

[5] P. de Forcrand and O. Philipsen, *Phys. Rev. Lett.* **105**, 152001 (2010).
 [6] K. Nagata and A. Nakamura, *Phys. Rev. D* **83**, 114507 (2011).
 [7] J. Takahashi, K. Nagata, T. Saito, A. Nakamura, T. Sasaki, H. Kouno, and M. Yahiro, *Phys. Rev. D* **88**, 114504

- (2013); J. Takahashi, H. Kouno, and M. Yahiro, *Phys. Rev. D* **91**, 014501 (2015).
- [8] C. R. Allton, S. Ejiri, S. J. Hands, O. Kaczmarek, F. Karsch, E. Laermann, C. Schmidt, and L. Scorzato, *Phys. Rev. D* **66**, 074507 (2002).
- [9] S. Ejiri, Y. Maezawa, N. Ukita, S. Aoki, T. Hatsuda, N. Ishii, K. Kanaya, and T. Umeda, *Phys. Rev. D* **82**, 014508 (2010).
- [10] G. Aarts, *Phys. Rev. Lett.* **102**, 131601 (2009).
- [11] G. Aarts, L. Bongiovanni, E. Seiler, D. Sexty, and I.-O. Stamatescu, *Eur. Phys. J. A* **49**, 89 (2013).
- [12] D. Sexty, *Phys. Lett. B* **729**, 108 (2014).
- [13] J. Greensite, *Phys. Rev. D* **90**, 114507 (2014).
- [14] G. Aarts, F. Attanasio, B. Jäger, E. Seiler, D. Sexty, and I.-O. Stamatescu, [arXiv:1411.2632](https://arxiv.org/abs/1411.2632).
- [15] M. Cristoforetti, F. Di Renzo, and L. Scorzato, *Phys. Rev. D* **86**, 074506 (2012).
- [16] H. Fujii, D. Honda, M. Kato, Y. Kikukawa, S. Komatsu, and T. Sano, *J. High Energy Phys.* **10** (2013) 147.
- [17] Y. Tanizaki, H. Nishimura, and K. Kashiwa, *Phys. Rev. D* **91**, 101701 (2015).
- [18] J. Condella and C. DeTar, *Phys. Rev. D* **61**, 074023 (2000).
- [19] Y. D. Mercado, H. G. Evertz, and C. Gattringer, *Phys. Rev. Lett.* **106**, 222001 (2011); C. Gattringer, *Nucl. Phys.* **B850**, 242 (2011); Y. D. Mercado and C. Gattringer, *Nucl. Phys.* **B862**, 737 (2012); Y. D. Mercado, H. G. Evertz, and C. Gattringer, *Comput. Phys. Commun.* **183**, 1920 (2012).
- [20] K. Langfeld and A. Wipf, *Ann. Phys. (Berlin)* **327**, 994 (2012).
- [21] J. Bloch, F. Bruckmann, and T. Wettig, *J. High Energy Phys.* **10** (2013) 140; J. Bloch, F. Bruckmann, and T. Wettig, *Proc. Sci.*, LATTICE (2013) 194 [[arXiv:1310.6645](https://arxiv.org/abs/1310.6645)]; J. Bloch and F. Bruckmann, *Phys. Rev. D* **93**, 014508 (2016); **93**, 039907 (E) (2016).
- [22] A. M. Polyakov, *Phys. Lett. B* **72B**, 477 (1978).
- [23] H. Kouno, Y. Sakai, T. Makiyama, K. Tokunaga, T. Sasaki, and M. Yahiro, *J. Phys. G* **39**, 085010 (2012).
- [24] Y. Sakai, H. Kouno, T. Sasaki, and M. Yahiro, *Phys. Lett. B* **718**, 130 (2012).
- [25] H. Kouno, T. Misumi, K. Kashiwa, T. Makiyama, T. Sasaki, and M. Yahiro, *Phys. Rev. D* **88**, 016002 (2013).
- [26] H. Kouno, T. Makiyama, T. Sasaki, Y. Sakai, and M. Yahiro, *J. Phys. G* **40**, 095003 (2013).
- [27] H. Kouno, K. Kashiwa, J. Takahashi, T. Misumi, and M. Yahiro, *Phys. Rev. D* **93**, 056009 (2016).
- [28] P. N. Meisinger and M. C. Ogilvie, *Phys. Lett. B* **379**, 163 (1996).
- [29] A. Dumitru and R. D. Pisarski, *Phys. Rev. D* **66**, 096003 (2002); A. Dumitru, Y. Hatta, J. Lenaghan, K. Orginos, and R. D. Pisarski, *Phys. Rev. D* **70**, 034511 (2004); A. Dumitru, R. D. Pisarski, and D. Zschiesche, *Phys. Rev. D* **72**, 065008 (2005).
- [30] K. Fukushima, *Phys. Lett. B* **591**, 277 (2004).
- [31] C. Ratti, M. A. Thaler, and W. Weise, *Phys. Rev. D* **73**, 014019 (2006); C. Ratti, S. Röbner, M. A. Thaler, and W. Weise, *Eur. Phys. J. C* **49**, 213 (2007).
- [32] E. Megias, E. R. Arriola, and L. L. Salcedo, *Phys. Rev. D* **74**, 065005 (2006).
- [33] T. Iritani, E. Itou, and T. Misumi, *J. High Energy Phys.* **11** (2015) 159; T. Misumi, T. Iritani, and E. Itou, in 33rd International Symposium on Lattice Field Theory, Lattice2015, 14-18 July 2015, Kobe International Conference Center, Kobe, Japan, [arXiv:1510.07227](https://arxiv.org/abs/1510.07227).
- [34] G. Aarts, F. Attanasio, B. Jäger, E. Seiler, D. Sexty, and I. O. Stamatescu, *Proc. Sci.*, LATTICE (2014) 200.
- [35] T. A. DeGrand and C. E. DeTar, *Nucl. Phys.* **B225**, 590 (1983).
- [36] F. Karsch and S. Stickan, *Phys. Lett. B* **488**, 319 (2000).
- [37] M. Alford, S. Chandrasekharan, J. Cox, and U.-J. Wiese, *Nucl. Phys.* **B602**, 61 (2001).
- [38] H. Fujii, *Phys. Rev. D* **67**, 094018 (2003); H. Fujii and M. Ohtani, *Phys. Rev. D* **70**, 014016 (2004).
- [39] J. D. Bjorken and S. D. Drell, *Relativistic Quantum Fields* (McGraw-Hill, New York, 1965).
- [40] A. Roberge and N. Weiss, *Nucl. Phys.* **B275**, 734 (1986).
- [41] L. McLerran and R. D. Pisarski, *Nucl. Phys.* **A796**, 83 (2007).
- [42] Y. Hidaka, L. McLerran, and R. D. Pisarski, *Nucl. Phys.* **A808**, 117 (2008).
- [43] C. N. Yang and T. D. Lee, *Phys. Rev.* **87**, 404 (1952); T. D. Lee and C. N. Yang, *Phys. Rev.* **87**, 410 (1952).
- [44] I. M. Barbour and A. J. Bell, *Nucl. Phys.* **B372**, 385 (1992); I. M. Barbour, S. E. Morrison, E. G. Klepfish, J. B. Kogut, and M.-P. Lombardo, *Phys. Rev. D* **56**, 7063 (1997); I. M. Barbour, S. E. Morrison, E. G. Klepfish, J. B. Kogut, and M.-P. Lombardo, *Nucl. Phys. B, Proc. Suppl.* **60A**, 220 (1998); I. Barbour, S. Hands, J. B. Kogut, M.-P. Lombardo, and S. Morrison, *Nucl. Phys.* **B557**, 327 (1999).
- [45] T. D. Cohen, *Phys. Rev. Lett.* **91**, 222001 (2003).